point towards the same observation. Temperature-dependent resistivity spectra of VCO films for each concentration were recorded for different cycles viz. heating cycle and cooling cycle. The spectra obtained in two different cycles did not overlap with each other considerably till around 60-70 ˚C. However, at temperatures higher than this the two cycles overlap. In addition, for pristine samples, two plateaux were observed which with the addition of Cr started vanishing and is almost gone with 30% Cr in the matrix. Our spectra could be divided into three different regimes viz. i) constant resistivity region from 320 K onwards, ii) exponential increasing region and iii) moderately increasing region. The second regime is decreasing at the expense of the third regime and is almost completely lost for the highest dopant concentration. One of the possible explanations could be the formation of the V-Cr complex which was averaging out the transport kinetics instead of being dominant from only a single type of charge carrier generator.

Table 1: Electrical resistivity ρ (Ω.cm), carrier concentration n (cm), Hall mobility μ (cm /V.s), Hall coefficient RH (cm /C) of the VCO films.

Sample Name	Resistivity, ρ (Ω.cm)	Carrier Concentration, n (cm^{-3})	Mobility, μ (cm^2 /V.s)	Hall Coefficient, R_H(cm^3 /C)
VO_2	2.27	1.90×10^{18}	1.45	3.29
$V_{0.95}Cr_{0.05}O_2$	1.90	8.77×10^{18}	0.98	1.31
$V_{0.9}Cr_{0.1}O_2$	0.86	7.44×10^{19}	0.69	0.84
$V_{0.8}Cr_{0.2}O_2$	0.18	4.14×10^{20}	0.07	0.13
$V_{0.7}Cr_{0.3}O_2$	0.15	8.23×10^{20}	0.06	0.01

Table 2. The switching parameters of the VCO films.

Sample Name	T_h(˚C)	T_c(˚C)	T_{MIT}(˚C)	ΔT (˚C)	FWHM (˚C)
VO_2	269.3	280.1	274.7	10.8	4.1
$V_{0.95}Cr_{0.05}O_2$	243.8	266.5	255.1	22.7	6.0
$V_{0.9}Cr_{0.1}O_2$	273.4	304.3	288.9	30.9	8.0
$V_{0.8}Cr_{0.2}O_2$	266.2	319.1	292.7	52.9	49.9
$V_{0.7}Cr_{0.3}O_2$	266.6	288.3	277.5	32.7	55.1

Based on the above-mentioned results one can discuss the effect of Cr doping on the structural and transport properties of our films. Results from the four-point probe resistivity measurements reveal the strong influence of Cr on the switching characteristics. The resistivity of VCO decreases with an increase in temperature. The VCO transform from an insulator to metal due to resistivity change induced by temperature. To study these features quantitatively and to determine precisely the full width at half maximum (FWHM ≈ΔH) and hysteresis width (ΔT), we plotted the derivatives of the resistivity variation curve, dlgρ/dT vs. T for both heating and cooling cycles. Several parameters are used to describe the phase transition properties of VCO films: (1) Th and Tc are the phase transition temperatures for the heating and cooling cycles, respectively, and are determined by calculating the corresponding minimum of dlg/dT for the two cycles; (2) TMIT is defined as the MIT temperature and was derived by averaging Th and Tc; (3) the ΔT is computed as the difference between Th and Tc; (4) the sharpness of the phase transition is represented by the FWHM of dlgρ/dT vs. T curve. These parameters for VCO thin films are presented in Table 2. TMIT of un-doped VO_2 (M1) was 274.7 K, lower than the TMIT standard value of 341 K. The low value of TMIT might be due to the large tensile strain and also from the existence of V^{5+} which is compared with that of the bulk VO_2. This tensile strain might be generated due to the cause of longer inter-planar distance in the un-doped sample compared to that of the bulk VO_2. A larger inter-planar distance in the VO_2 crystal structure suggests a longer V-V distance, indicating a weaker interaction between V-V bonds. In other words, in the un-doped sample, the energy required to trigger the semiconductor–metal phase transition is lower than in the standard VO_2. The TMIT of Cr-doped VO_2 thin films initially drops and reach a temperature of 255.1 K at the Cr concentration of 5%. When Cr concentration increased, the TMIT further increased to 292.7 K. The lower MIT in 5% could be observed due to the defect scattering and poor crystallinity while 10-20% doping of Cr^{3+} has dramatically raised the TMIT to 37.6 K. As 10-20% Cr^{3+} doped into VO_2 lattices and it replaces V^{4+} to form Cr^{3+}-V^{4+} bonds result in distorted lattices around Cr

ions. To overcome such distortions and activate the MIT, more energy is required which resulted in a significant enhancement of TMIT [1].

It is seen from measurement that the difference of FWHM between Cr-doped samples and un-doped samples is not obvious. The doped, as well as the un-doped samples, behave similarly in terms of stable performance and rapid response to temperature. In addition, the FWHM steadily increases with Cr-doping. Hence, the transition became less abrupt, extending over a wide range of temperatures. The ΔT is generally observed to be narrow with Cr addition. Finally, it is observed that with increasing Cr concentration, ΔT first increases and then decreases. A lower ΔT implies that the sample can respond quickly to temperature variations. Although Cr doping increases the hysteresis width slightly in this work, compared with the VCO thin films reported elsewhere [1], the hysteresis width has little effect on Cr concentration. Therefore, Cr doping can effectively modify the thermochromic properties of VO_2. According to Sun *et al* [2], the smaller cell volume and larger b angle can result in a decrease in TMIT. Therefore, the Cr-doping- induced lattice perturbation is one of the most dominant reasons for the change of T_C.

REFERENCES:

[1] Y. F. Wu, C. W. Zou, L. L. Fan, Q. H. Liu, S. Chen, W. F. Huang, Z. Y. Wu, F. H. Chen, G. M. Liao. Sci Rep. **5**, 9328(2015).
[2] C. Sun, L. Yan, B. Yue, H. Liu and Y. Gao. J. Mater Chem C. **2**, 9283(2014).

5.2.4 A comparative study of 100MeV Ag^{9+} ion irradiation induced modifications in structural, optical, and electrical properties of α- Al_2O_3 by fluence variation

Collin B Nettar[1], R. N Bhowmik[1*], K. Asokan[2], R.C Meena[2], and S.A Khan[2]

[1]*Department of Physics, R.V Nagar, Pondicherry University, Kalapet-605014, India.*
[2]*Material Science Division, Inter-University Accelerator Centre, Aruna Asaf Ali Marg, New Delhi-110067, India.*

In order to tailor the Ferroelectric properties in high conductive and low polarizable dielectric oxides, we have synthesized Al $(OH)_3$ via chemical precipitation method [*for details, see Ceramic. Inter. 48 (2022) 10677].* The as-prepared powder was heated in the temperature range 250 ˚C-1250 ˚C for studying structural, optical, electrical, ferroelectric properties. SXRD confirms the polymorphic phases on increasing heat treatment. The boehmite (γ-AlOOH) and α- Al_2O_3 phase showed Raman active modes, whereas meta-stable multi-phased structure shows minor Raman peaks. The analysis of UV-Visible shows two optical bandgap energy values in a high energy range of 4.50- 4.73eV and the low energy range of 3.06-3.84eV. The smaller optical band attributes the defect induced additional electronic state between valence and conduction band. The electronic charge conduction in metastable multi-phased samples was fitted with the Space Charge Limited Conduction (SCLC) mechanism, whereas the sample at 1250 ˚C shows Schottky Emission (SE) mechanism. σ(T) and ε_r curves of the sample exhibited an intermediate metal-like state between low-temperature semiconductor to high-temperature semiconductor states. The nature of the cooling mode of the temperature variation differed from the warming mode due to the thermal cyclic effect of electrical properties [*for details, see Inorg. Chem. 59 (2020) 6763].* A correlation in the temperature variation of dc conductivity, dielectric constant, and P(E) loop parameters confirms that the observed electric polarization in Al_2O_3 samples exhibited signature of Ferroelectric properties [*for details, see Ceramic. Inter. 48 (2022) 10677]*.

In order to investigate the effects of the swift heavy ion (SHI) irradiation on the structural, optical, electrical and magnetic properties of Bulk Al_2O_3 and Al_2O_3, Ga- doped Al_2O_3 thin-films, we have deposited the pristine and $Al_{1.5}Ga_{0.5}O_3$ thin films on Quartz., Si<100> wafer and Alumina <0001> using Electron Beam Evaporation method. The base pressure was maintained at 4.2×10^{-7} mbar prior to deposition of the films and working pressure was maintained at 3.5×10^{-5} mbar and the substrate temperature 550 ˚C. After phase analysis of the bulk Al_2O_3 samples were irradiated using 15UD Pelletron tandem accelerator at IUAC, New Delhi with 100MeV Ag^{9+} ions with ion fluence of 1×10^{11} ions/cm^2, 1×10^{12} ions/cm^2, 5×10^{12} ions/cm^2, 1×10^{13} ions/cm^2 respectively with 1 pnA current. All the samples were fixed to the target ladder placed inside the high vacuum ($\sim10^{-6}$ torr) chamber during irradiation. Irradiation was performed in the direction perpendicular to the sample surface. The ion beam was focused to a spot of 10 mm diameter and then scanned over an area of 1×1 cm^2 using a magnetic scanner to cover the complete sample surface for uniform irradiation. XRD patterns at room temperature confirmed the Rhombohedral structure (space group R-3c) for the pristine and irradiated samples. Raman spectra indicated some microstructural changes in the irradiated samples. The FE-SEM images indicated a change in the surface morphology of the irradiated sample with respect to the pristine sample. XPS spectra confirmed the presence of the Al^{3+} state of Al_2O_3 and revealed the presence of oxygen vacancy in the system. The optical bandgaps are systematically reduced with the increase of ion fluences. The electrical conductivity measurement in the temperature range 300 K-450 K showed a transformation from a metal- like behavior (low-temperature region) to a semiconductor-like (high-temperature region) behavior. The electrical conductivity at room temperature (300 K) decreased while the electrical conductivity increased at 450 K with an increase of fluence from the irradiated samples [Manuscript writing is under process].

REFERENCES

[1] Collin B Nettar, R.N Bhowmik, A.K Sinha, Ceramic. Inter. **48**, 10677 (2022).

[2] R.N Bhowmik, P.D Babu, A.K Sinha, A.Bhisikar, J. Appl. Phys. **124** , 164105(2018).

5.2.5 Thickness dependent surface properties and scaling law of nano-dimensional SnTe thin films

G. Maity,[1] R. P. Yadav,[2] R. Singhal,[3] I. Sulania,[4] A. K. Mittal,[5] Dhirendra. K. Chaudhary,[6] D. Kanjilal,[4] and Shiv. P. Patel[1]

[1]*Department of Pure and Applied Physics, Guru Ghasidas Vishwavidyalaya (A Central University), Bilaspur 495009, India*

[2]*Department of Physics, Deen Dayal Upadhyay Govt. PG College, Prayagraj-221508, India*

[3]*Department of Physics, Malaviya National Institute of Technology, Jaipur-302017, India*

[4]*Inter University Accelerator Centre, Aruna Asaf Ali Marg, New Delhi 110067, India*

[5]*Physics Department, University of Allahabad, Allahabad-211 002, India*

[6]*Centre for Renewable Energy, Prof. Rajendra Singh (Rajju Bhaiya) Institute of Physical Sciences and Research, V. B. S. Purvanchal University, Jaunpur 222003, India*

A topological crystalline insulator (TCI) such as tin selenide (SnTe) is a direct narrow band gap (i.e. 0.35 eV) semiconductor with rock salt structure. SnTe has wide applications in thermoelectric devices, mid-infrared (MIR) detectors, and photo detectors.[1] In the present work, the effects of film thickness on scaling law and surface properties (i.e. morphologies and optical properties) of SnTe thin films has been investigated. The SnTe thin films of different thicknesses are prepared by means of e-beam evaporation technique. The surface morphology of each film is captured by atomic force microscopy (AFM) as well as scanning electron microscope. The crystallinity of the films is found to increase with increasing film thickness, as confirmed by x-ray diffraction and Raman measurements. Fractal analysis is performed on AFM images to investigate the irregularity of surfaces. It is found that the surface of thicker sample is rougher than the thinner sample and the autocorrelation function is applied to investigate the self-affine fractal nature of surfaces. The average roughness, interface width, lateral correlation length, local surface slope and fractal dimension increased with film thickness. The value of roughness exponent, growth exponent, dynamic exponent, and steepening exponent are calculated and found to be $\alpha = 0.76 - 0.96$, $\beta = 0.75$, $z = 1.92$, and $\lambda = 0.35 - 0.25$, respectively. The scaling exponents together with the other parameter like the local surface slope, indicate that the growth is quasi-3D island/mound type with rapid surface roughening behavior and obey anomalous scaling. The multiple scattering cross-sections of light together with Fourier transform infrared spectroscopy data analyses suggest that the higher crystalline film with a smaller number of defects are infrared sensitive which may be most suitable for advance mid-infrared applications.[2]

REFERENCES

[1] M. P. Smylie, K. Kobayashi, T. Takahashi, C. Chaparro, A. Snezhko, W. K. Kwok, and U. Welp, Phys. Rev. B **101**, 094513 (2020).

[2] G. Maity, R. P. Yadav, R. Singhal, I. Sulania, A. K. Mittal, Dhirendra. K. Chaudhary, D. Kanjilal, and Shiv. P. Patel, J. Appl. Phys. **130**, 175306 (2021).

5.2.6 Structural and phase transformation studies of 1.4 MeV Kr ion beam irradiated zirconia thin films

Ankit Kumar[1], Pravin Kumar[2], A S Dhaliwal[1]

[1]*Department of Physics, Sant Longowal Institute of Engineering and Technology, Longowal 148106 (Punjab),*

[2]*Inter University Accelerator Centre, Aruna Asaf Ali Marg, New Delhi-110067, India*

The thin films of zirconia were synthesized on the silicon substrates (size of 1.0 cm x 1.0 cm) using an electron beam deposition technique. Some of the films were annealed at 800 ˚C for 2 hours at a heating and cooling rate of 2 ˚C/min and 3 ˚C/min, respectively in the air to improve their crystallinity. The as-deposited films at room temperature and those annealed at 800 ˚C, both types, were irradiated with a 1.4 MeV Kr ion beam at three different ion fluences viz. 7.0×10^{14}, 1.0×10^{15}, 3.0×10^{15} ions/cm^2, respectively using the Low Energy Ion Beam Facility (LEIBF) at Inter University Accelerator Centre (IUAC), New Delhi, India [1]. The beam current on the target (during irradiation) was maintained at ~ 1.0 μA. The vacuum in the irradiation chamber was at ~ 5.7 x 10^{-7} mbar. The influence of irradiation on the structural properties and phase transformation behaviour of thin films is examined by Bruker D8 advance X- ray Diffractometer (XRD). The X-ray diffraction analysis of as-deposited thin film showed amorphous nature and the annealing of it at 800 ˚C confirmed the development of the monoclinic phase. The ion beam bombardment with increasing fluence resulted the evolution of a cubic phase in as-deposited amorphous zirconia films as shown in fig. 1(a). Further, annealed films undergo a monoclinic to cubic phase transformation as shown in fig. 1(b). The cubic zirconia films find wide applications in developing new technologies for mankind [2-4] and

therefore, the stabilizing cubic phase in zirconia is an interesting and challenging task. The present studies on phase formation/stabilization in zirconia showed that ion beam bombardment is a fascinating tool for materials synthesis and their modifications.

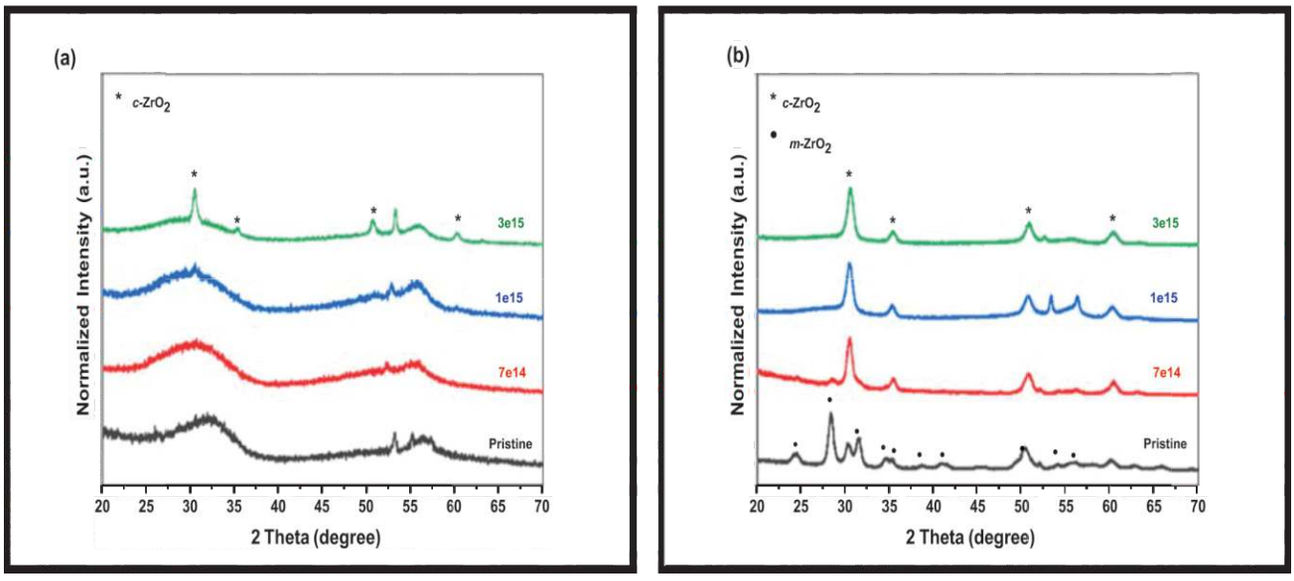

Fig.1. XRD spectra of the (a) as-deposited films (b) annealed at 800 ˚C zirconia thin films irradiated with 1.4 MeV for Kr ions at different fluences.

REFERENCES:

[1] P. Kumar, G. Rodrigues, P.S. Lakshmy, D. Kanjilal, B.P. Singh, R. Kumar, Development of metallic ion beams using ECRIS, Nucl. Instruments Methods Phys. Res. Sect. B Beam Interact. with Mater. Atoms. **252**, 354–360(2006).

[2] M. Keshavarz, M.H. Idris, N. Ahmad, Mechanical properties of stabilized zirconia nanocrystalline EB-PVD coating evaluated by micro and nano indentation, J. Adv. Ceram. **2**, 333–340(2013).

[3] C. López-Gándara, F.M. Ramos, A. Cirera, YSZ-Based Oxygen Sensors and the Use of Nanomaterials: A Review from Classical Models to Current Trends, J. Sensors., 1–15(2009).

[4] M. Streit, W. Wiesenack, T. Tverberg, C. Hellwig, B.C. Oberländer, Yttrium stabilised zirconia inert matrix fuel irradiation at an international research reactor, J. Nucl. Mater. **352** , 349–356(2006).

5.2.7 Tuning of the Structural, Morphological, Dielectric, and Magnetoresistance Properties of Gd_2NiMnO_6 Double Perovskite by Ca Doping

Mohd Ikram and Nazima Nazir

Department of Physics, Solid State Physics Research Lab, National Institute of Technology, Srinagar, J&K, 190006, India.

The effect of replacing Gadolinium with Calcium in site A of the Gd_2NiMnO_6 perovskite on the structural, dielectric, morphological, and magnetoresistance properties was examined in this paper. The materials were synthesized using the solid-state process. X-Ray Diffraction was adopted to determine the phase of the samples that revealed a monoclinic structure along with P21/n space group verified using Rietveld refinement. Scanning Electron Microscope imaging of the samples shows the grain size reduction after doping with Ca^{2+} ions. The grain and grain boundaries were found to have a significant influence on the temperature and frequency dependence of the dielectric properties. A huge enhancement in dielectric constant accompanied with diminished dielectric loss was found by increasing the concentration of dopant. Also, an eligible effect on magnetoresistance by applying a high magnetic field was found. However, the resistivity happened to be increased tremendously with doping. This improvement in dielectric properties indicates that these samples can be used in high-frequency applications. XRD, SEM, and dielectric measurements were carried out at IUAC, New Delhi [1].

REFERENCES:

[1] Nazima Nazir and Mohd. Ikram "Tuning of the Structural, Morphological, Dielectric, and Magnetoresistance Properties of Gd_2NiMnO_6 Double Perovskite by Ca doping", Physica B **632**, 413734 (2022) [I.F. = 2.40].

5.2.8 Investigating the Structural and Dielectric Properties of $CoFe_{2-x}Ni_xO_4$ Spinel Ferrite.

Mohd Ikram and Gulzar Ahmad Lone

Department of Physics, Solid State Physics Research Lab, National Institute of Technology, Srinagar, J&K, 190006, India.

In order to investigate the structural and dielectric properties of the pristine and Ni doped $CoFe_2O_4$ spinal Ferrite, the samples were synthesized using a solid-state reaction approach. A single-phase FCC cubic spinel structure with space group Fd-3m was confirmed for all the prepared materials with the help of Rietveld refinement. The cationic distribution indicates a decrease in the occupancy of Fe^{2+} and the corresponding increase of that of Ni^{2+}. The microstructural analysis and the elemental composition analysis were carried out using SEM and energy dispersive spectroscopy (EDS) respectively. For all samples the temperature-dependent dielectric characteristics were investigated, revealing the presence of orientation and interfacial polarization. The dielectric constant is temperature independent until it reaches around 270K, after which it begins to increase with increasing temperature. And this temperature starts decreasing for higher doping concentrations. Also, $CoFe_{1.9}Ni_{0.9}O_4$ was seen to have strong relaxation behavior and low dielectric loss. The low dielectric loss of $CoFe_{1.9}Ni_{0.9}O_4$ makes it useful at higher frequencies in electrical circuits that faces the challenges of high-temperature rise [1].

REFERENCES:

[1] Gulzar Ahmad lone and Mohd. Ikram "Investigating the Structural and Dielectric Properties of CoFe2-xNixO4 Spinel Ferrite" Journal of Alloys and Compounds, **908**, 164589(2022) [I.F. = 5.316].

5.2.9 The Effects of Swift Heavy Ion Irradiation on Silicon NPN Transistors

T. M. Pradeep[1], Vinayakprasanna N. Hegde[2], Arshiya Anjum[1], N. Pushpa[3], Ambuj Tripathi[4] and A. P. Gnana Prakash[5]

[1]*Department of Biomedical and Robotics Engineering, Mysore University of School of Engineering, Mysuru-570 006, India.*

[2]*Department of Physics, Vidyavardhaka College of Engineering, Gokulam, Mysuru-570 002, India.*

[3]*Department of PG Studies in Physics, JSS College, Ooty Road, Mysore-570 025, India.*

[4]*Inter University Accelerator Centre, Aruna Asaf Ali Marg, New Delhi-110 067, India.*

[5]*Department of Studies in Physics, University of Mysore, Manasagangotri, Mysore-570 006, India.*

Corresponding author: gnanaprakash@physics.uni-mysore.ac.in

In space environment there are numerous electronic components composed of silicon integrated circuits fabricated in bipolar and bipolar complementary metal oxide semiconductor (BiCMOS) processes. Bipolar junction transistors(BJTs) have an important application in these integrated circuits, and are susceptible to both ionization damage and displacement damage. When semiconductor devices and circuits are operating in radiation environment, devices shows significant degradation in electrical characteristics and affect the performance of the electronic circuits [1]. Therefore, in the present study the transistors were exposed to 80 MeV nitrogen ions (N^{6+}) and 100 MeV phosphorous (P^{7+}) ions in 15 UD 16 MV Pelletron Accelerator at Inter University Accelerator Centre (IUAC), New Delhi, India. The irradiation was performed at room temperature with the dose ranges from 600 krad (Si) to 100 Mrad (Si) for both ions. All the ion irradiations were done *in-situ* in the experimental chamber maintained at a vacuum of 10^{-7} mbar and all the terminals of the transistors were grounded during the irradiation. The *in-situ* electrical measurements were carried after exposure to different total doses. In case of *in-situ* irradiation, all the ion fluence dependent measurements are done on the same device by incrementally increasing the ion fluence under same irradiation test conditions so that there will be no variation in the results due to variation in initial parameters of different device and also avoided the effects of post irradiation time annealing of the defects caused by ion beam irradiation in the device. The key electrical parameters like Gummel characteristics, excess base current ($\Delta I_B = I_{Bpost} - I_{Bpre}$), dc current gain ($h_{FE}$), output characteristics (I_C-V_{CE}) and collector saturation current (I_{CSat}) were characterized. Some of the results are presented here.

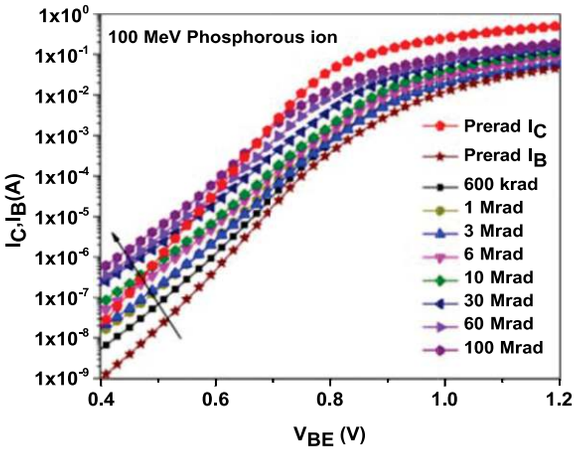

Fig. 1: The Gummel characteristics of 100 MeV P^{7+} ion irradiated transistor

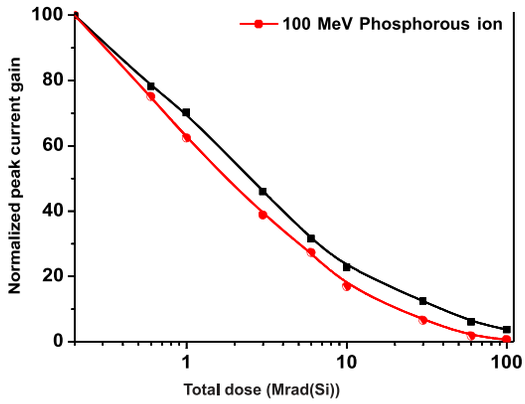

Fig. 2: The normalized hFE as a function of dose

REFERENCES

[1] T. M. Pradeep, Vinayakprasanna N. Hegde, N. Pushpa, A. Tripathi, K. Asokan, and A. P. Gnana Prakash. Radiat. Eff. Defects Solids. **174**, 859(2019).

5.2.10 50 MeV Lithium Ion Irradiation Studies on 200GHz SiGe HBTs at Low Temperature

V. N. Hegde[1], T. M. Pradeep[2], Arshiya Anjum[2], N. Pushpa[3], John D. Cressler[4], Ambuj Tripathi[5] and A. P. Gnana Prakash[2,*]

[1]*Department of Physics, Vidyavardhaka College of Engineering, Gokulam, Mysuru-570 002, India.*
[2]*Department of Studies in Physics, University of Mysore, Manasagangotri, Mysuru-570 006, India.*
[3]*Department of PG Studies in Physics, JSS College, Ooty Road, Mysore-570 025, India.*
[4]*School of Electrical and Computer Engineering, Georgia Institute of Technology, Atlanta, GA, 30332 -0250, USA.*
[5]*Inter University Accelerator Centre, Aruna Asaf Ali Marg, New Delhi-110 067, India.*
Corresponding author: gnanaprakash@physics.uni-mysore.ac.in

The SiGe HBT Bi-CMOS technology has come out as a fundamental building block for many extreme environment electronic applications, including at cryogenic temperatures, elevated temperatures and radiation-harsh environments. Due to band-gap engineering, the performance of these devices is superior at cryogenic temperature than that at 300K. Because of these advantages of SiGe HBTs, the space communities are considered using these devices in space exploration programs [1]. In space, the electronic systems have to work in harsh environments such as, under irradiation and at extreme temperatures. For such applications, one must demonstrate the reliability of SiGe HBTs under the exposure to very high radiation dose levels while operating in a wide temperature range. Hence, experimental characterizations and reliability testing of these devices at extreme temperatures are needed. Therefore, systematic investigations on the 50 MeV lithium ion irradiation effects on SiGe HBTs at both low temperature (150K) and room temperature (300K) are carried out. The 200GHz SiGe HBTs procured from IBM, USA are employed for this study. The devices were subjected to 50 MeV lithium ions in 15UD 16MV Pelletron Accelerator at Inter University Accelerator Centre (IUAC), New Delhi, India. The devices were irradiated at temperatures 150K and 300K with ion dose range from 1 to 30 Mrad. In order to achieve a temperature of 150K, liquid nitrogen was poured in to a sample holder. The SiGe HBTs were placed on the copper strip on the sample holder to reduce the temperature gradient and the temperature of the device was measured using a temperature sensor during the ion irradiation. The I-V characteristics of the irradiated and pre-irradiated devices were carried out at 300K by using Keithley 2636A dual source meter. The different DC parameters namely, Gummel characteristics, normalized base current (I_{Bpost}/I_{Bpre}), excess base current (ΔI_B), current gain (h_{FE}), avalanche multiplication (M-1) and the output characteristic (I_C-V_{CE}) were measured. Some of the results are presented here.

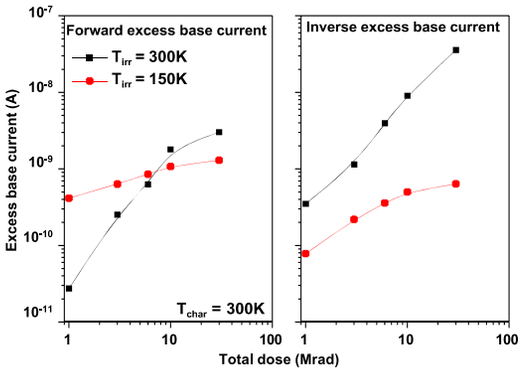

Fig. 1: The ΔI_B as a function of the total dose

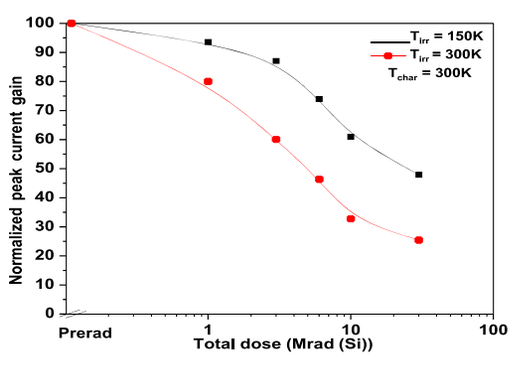

Fig. 2: The normalized h_{FE} as a function of dose

The variation in forward and inverse mode ΔI_B for lithium ions irradiated SiGe HBTs is shown in Fig. 1. Both forward and inverse excess base currents increased after lithium ion irradiation at both temperatures. Forward ΔI_B of HBTs irradiated at 300K increased around three orders of magnitude. However, low temperature irradiation causes less increase in the forward ΔI_B. A similar trend can be observed in inverse mode ΔI_B. It is also evident from the figure that increase in inverse ΔI_B is more compared to forward ΔI_B. The normalized h_{FE} extracted at collector current of 1μm for ion irradiated SiGe HBTs is depicts in Fig. 2. The SiGe HBT irradiated at 150K shows less decrease in h_{FE} (at $I_C=1_{\mu m}$) than SiGe HBTs characterized at 300K. After the 30 Mrad of the total dose, degradation in h_{FE} (at $I_C=1_{\mu m}$) is around 53% at 150K and around 75% at 300K irradiation. At low temperatures, carrier mobility increases, reduction in minority carrier lifetime is not significant, built-in voltage increases, mean energy required for hole-electron pair creation increases and energy gap also increases. All these factors together cause less degradation at low temperature ion irradiation.

REFERENCES:

[1] J. D. Cressler, IEEE Trans. Device Mater. Reliab. **10**, 437 (2010).

5.2.11 Origin of intense blue-green emission and bandgap engineering in $SrTiO_3$ thin films using ion-beam techniques: An synchrotron-based spectroscopic study

Vishnu Kumar[1], Anuradha Bhogra[2] Manju Bala[1], Hung-Wei Kuo[3], S. C. Haw[3], C. L. Chen[3], C. L. Dong[4], K. Asokan[2], and S. Annapoorni[1]

[1]*Department of Physics and Astrophysics, University of Delhi, Delhi, 110007, India*
[2]*Inter-University Accelerator Centre, Aruna Asaf Ali Marg, New Delhi, 110067, India*
[3]*National Synchrotron Radiation Research Center, Hsinchu, 30076, Taiwan*
[4]*Department of Physics, Tamkang University, Tamsui 25137, Taiwan*

STO thin films were deposited on quartz substrates using a commercial STO target of 2 mm thickness and 5 cm diameter by radio frequency (RF) magnetron sputtering (HIND HIVAC, Model 12" MSPT) in the presence of oxygen (20%) balanced with argon gas. The cleaned quartz substrates of dimensions 10 mm × 10 mm × 2 mm were used to deposit STO thin films. These films were annealed at 750 °C for 5 h in a horizontal tubular furnace in the ambient of $Ar+O_2$ (20%) gas. The thickness of the films was determined to be ~220 nm. These pristine films were implanted with 100 keV N ion beam using the low energy ion beam facility (LEIBF) housed in Inter-University Accelerator Centre (IUAC), New Delhi with different fluences viz. ~5×10^{14}, ~1×10^{15}, ~5×10^{15}, and ~1×10^{16} ions/cm^2. For the structural characterization, synchrotron glancing incidence X-ray Diffractometer (GIXRD) operated at 13 keV was used at MCX Beamline, Elettra Sincrotrone Trieste, Italy. Further, the samples were characterized by synchrotron PL spectroscopy at TLS-03A1, and XAS at TLS-20A1 & TLS- 17C1 beamlines of National Synchrotron Radiation Research Center (NSRRC), Hsinchu, Taiwan. The XRD pattern shows a shift in reflections at lower N ion fluences and the amorphization of the films at higher fluences. A disordered phase induced by implantation in the STO films leads to an intense blue-green emission due to oxygen (O) vacancies and N (2p) bound states. A schematic diagram of energy levels has been proposed to explain the origin of PL emission. The XANES spectra at Ti *K*-edge reflect a change in the valency of Ti ions and the local atomic structure of ordered and disordered phases of STO with an increase in N ion fluence. The splitting of peak assigned to e_g orbitals, and discrepancy in ratio dz^2/dx^2-y^2 observed in the Ti *L*-and O *K*-edge spectra confirm a distortion in TiO6 octahedral structure and modifications in O 2p-Ti 3d hybridization states. The synchrotron-based techniques reveal that N ion implanted STO can be a good photo luminescent material exhibiting a variety of emissions through bound states of O vacancies and implanted N ions [1].

Another set of STO films were deposited on cleaned quartz substrates using the Radio Frequency (RF) magnetron sputtering technique. The thickness of the films was determined to be ~750 nm. These pristine films were irradiated at IUAC, New Delhi, India with 125 MeV silver (Ag^{+9}) beam at different ion fluences of 1×10^{11}, 1×10^{12}, and 5×10^{12} ions/cm^2. The structural studies were carried out using the synchrotron Glancing Incidence X-Ray Diffractometer (GIXRD) at the MCX beamline at Elettra Sincrotrone Trieste, Italy. The diffraction measurements were performed using 13 keV energy of the X- ray source. The surface morphology of the films was examined using a Field Emission Scanning Electron Microscope (FESEM - Zeiss GeminiSEM 500) operated at 30 kV. The UV-visible absorbance spectra were recorded using a UV-Visible spectrophotometer (SHIMADZU UV-2600). The X-ray Absorption Near- Edge Structure (XANES) Spectra at Ti *K*-edge were recorded in fluorescence mode at the TLS-17C1 Wiggler beamline at National Synchrotron Radiation Research Center (NSRRC), Hsinchu, Taiwan. Engineering the opticalbandgap of metal oxides is essential for optoelectronic and photocatalytic applications. This study reports the application of electronic excitations, induced by 125 MeV Ag ions, in tuning the bandgap of $SrTiO_3$ films in the range of 2.93-3.78 eV and their correlation with the synchrotron-based X-ray diffraction pattern and X-ray absorption spectra (XAS). The pre-edge spectral features in the XAS at Ti *K*-edge show significant variation in the